Heliyon 10 (2024) e23376

Contents lists available at ScienceDirect

Heliyon

journal homepage: www.cell.com/heliyon

Effect of shell spacing on mechanical behavior of multi-span soil-steel composite structure

Alemu Mosisa Legese [a,b,*], Adrian Różański [a], Maciej Sobótka [a]

[a] Wrocław University of Science and Technology, Faculty of Civil Engineering, Wybrzeże Wyspiańskiego 27, 50-370, Wroclaw, Poland
[b] Faculty of Civil and Environmental Engineering, Jimma Institute of Technology, Jimma University, Jimma P.O. Box 378, Ethiopia

ARTICLE INFO

Keywords:
Moving load
Multi-span
Soil-steel composite structure
Spacing

ABSTRACT

This study analyses the effect of lateral shells on central shell at a different spacing in a multi-span soil-steel composite structure subjected to quasi-static moving loads. The displacements and internal forces of the central shell during consecutive truck passages over the structure are investigated by finite element (FE) analysis. Field measurements from a site in Niemcza, Poland, are used to calibrate input parameters. Next, the simulations for different spacing between the shells are investigated. The backfill soil is modeled as elastic-perfectly plastic, while the shells and sheet piles are linear elastic. The non-linear contact zone between the shell and the soil backfill is assumed to reflect an elastic-plastic constitutive model. The analysis reveals that both vertical and horizontal displacements increase significantly when the ratio of shell spacing to span length is less than 0.5. Maximum stress occurs when the shells are placed adjacent to each other, i.e., without spacing. The stress is almost doubled in this position compared to the reference case—a single-span structure. The shifting of extreme deflections and stress is observed in the direction of truck movement. Nevertheless, the influence of lateral shells on the central shell's performance under moving loads is nearly negligible when the spacing-to-span ratio exceeds 0.5.

1. Introduction

The soil steel composite structure (SSCS) is a composite structure in which a flexible buried steel plates interacts with the surrounding backfill and creates a composite effect [1,2]. The performance of SSCS depends on the interaction of two main elements: the steel plate and the backfill soil. The steel plate of the SSCSs alone is relatively weak under external loads. However, due to arching phenomena in the backfill, the composite structure can carry large loads despite the use of much lighter structural elements compared to other types of structures [3–6]. Thus, the synergistic interaction between soil and steel within such structures offers enhanced load-bearing capacity. These structures have undergone significant development over the past decades and have grown in size and number as more knowledge in this sector has been developed through large-scale tests and simulations [7,8]. Today, this type of structure is increasingly being used in road, railway, tunneling, and animal overpass projects as an alternative to conventional type bridges, for example, reinforced concrete (RC) slab bridges [9–12]. Recent evidence suggests that SSCS is relatively easy to construct [13–15] and more economical [14,16,17] than its conventional counterparts, e.g., concrete bridges. The lack of expansion joints [18, 19] and the possibility of forming on weak ground [14,20] are other benefits of such structures (see Fig. 4).

* Corresponding author. Wrocław University of Science and Technology, Faculty of Civil Engineering, Wybrzeże Wyspiańskiego 27, 50-370, Wroclaw, Poland.
E-mail address: alemu.legese@pwr.edu.pl (A.M. Legese).

https://doi.org/10.1016/j.heliyon.2023.e23376
Received 24 July 2023; Received in revised form 24 November 2023; Accepted 1 December 2023
Available online 9 December 2023

Extensive research has been carried out to understand the mechanical behavior of SSCSs under various loading conditions, e.g., under static load [21,22], semi-static load [19,23–25], dynamic load [10,26,27], and seismic excitation [9,28,29]. Furthermore, several attempts have been made in both field tests [16,30,31] and numerical simulation [32–34] to investigate the response of SSCSs under ultimate loading conditions.

The arrangement of spans in multi-span SSCS holds a critical role in dictating their mechanical behavior. This pivotal aspect, including the spacing between individual shells, profoundly influences the load distribution, stress propagation, and overall structural response. Example of multi-spans soil steel composite structure is shown in (Fig. 1).

Understanding the intricate interactions between shell spacing and mechanical behavior is paramount for the informed design and robust performance of these composite systems.

The most accurate sources of information on the mechanical response of SSCS are full-scale tests [19]. They allow one to measure the displacements in the shell and determine the internal forces. However, theoretical models are required for design purposes. The mechanical response of such a structure depends on different conditions, like the steel plate geometry, the height of the soil cover, span (single-span or multi-span), and others. Conducting full-scale tests is expensive; mainly for multi-span, it becomes more expensive. Thus, numerical analysis is the appropriate method for studying the impact of interactions between adjacent shells on the mechanical behavior of the composite structure under varying loading conditions.

The behavior of multi-span SSCS during construction and service stages has been studied by many scholars. Numerical simulation on performance of multi-span SSCS during construction and operation stage under vehicle load conducted by Ref. [35] and concludes that stress and deformation initially increase rapidly with load cycles, stabilizing afterward. The influence of multi-arch culvert spacing and mechanical behavior under seismic conditions was analysed by Ref. [36] through numerical. The results indicate that with narrow element spacing, the overall stiffness of the soil and culvert increases. The influence of multi-arch culvert spacing through dynamic finite-element analysis by Ref. [37] and found that when the spacing between arch culverts is close, the increase in ground stress is observed while volumetric strain is limited.

The numerical analysis on two span SSCS under railway load was analysed in the work of [38]. In their analysis, the influence of interactions between adjacent shells on the values of internal forces was demonstrated. In the study, three different structural models were prepared, each with varying spacings between adjacent shells: 0.72 m, 1.3 m, and a model without an adjacent shell (single shell). The analysis aimed to investigate how these different configurations influence the cross-sectional forces and stress levels within the structure. The authors' findings unequivocally confirm that the spacing between adjacent shells has a substantial impact on reducing cross-sectional forces occurring in the structure. This result underscores the importance of considering the arrangement of adjacent shells in the design and analysis of shell structures. When comparing the first model (0.72 m spacing) with the second model (1.3 m spacing), it becomes evident that significantly lower values of forces were obtained as the spacing increased. This trend suggests that a greater distance between adjacent shells leads to a more efficient distribution of loads and consequently reduces the cross-sectional forces experienced by the structure. Furthermore, the authors compared the models with adjacent shells at different spacings to a model with a single shell, where there is no adjacent shell. The results revealed that the stress levels in the structure were significantly impacted by the presence and spacing of the adjacent shell:

When the adjacent shell was spaced at 0.72 m, the stress increased by a substantial 90 % compared to the single-shell configuration. This indicates that a closer spacing between shells can lead to higher stress levels, potentially affecting the structural integrity. Similarly, when the adjacent shell was spaced at 1.3 m, the stress increased by 30 % compared to the single-shell configuration. While this increase is less pronounced than in the closer spacing scenario, it still highlights the importance of considering the spacing between adjacent shells in structural analysis and design. These findings have practical implications for the design and engineering of shell structures. They emphasize the significance of optimizing the spacing between adjacent shells to achieve desired structural performance, minimize forces, and ensure structural stability. The choice of shell spacing should be carefully considered based on the specific requirements and loading conditions of the structure.

However, Research on three-span SSCS behavior under cyclic quasi-static moving loads with variable lateral shell spacing is currently limited.

Fig. 1. Example of Multi-span Soil steel composite structure [5].

This study presents two-dimensional finite element analyses to investigate the influence of lateral shells on the mechanical behavior of the central shell at various inter-shell spacings within a multi-span SSCS when subjected to quasi-static moving loads. For the analysis, an experimentally validated computational model was developed using non-linear finite element method (FEM) and implemented in the Zsoil FEA numerical program.

The paper is structured as follows: The second section of this paper gives a description of the behaviour of the structure under live load field test, testing procedure, and input parameters. The third section of this paper describes numerical modelling and simulation procedures. The result of the simulations was described in fourth section 4. Subsequent fifth section 5 reflects the discussion on the obtained simulation results. Finally, the paper concludes with a summary and conclusion.

2. The behaviour of the structure under live load

The structure tested by Ref. [3] a single-SSCS with 5.0 m span and 1.85 m height, built near Niemcza, Poland. The flat steel shell, shaped like a circular arch, has a thickness of 23.0 mm. The cross-section of the tested structure is shown in Fig (2). The measuring base was adjusted to load schemes by a truck and the shell's configuration. The measurements were done at ten reference points on the bottom surface of the shell by setting sensors in longitudinal and transverse directions.

2.1. Testing procedure

The experimental test is conducted by moving the dumper truckload on the bridge. During this experimental test, displacements and strain increments are recorded on the bottom of the shell under a moving truck. The loading arrangement is shown in Fig. 3(a–b).

During the test, the truck crosses the bridge while moving to the left, then turns around and drives to the right. The driving was accomplished in a quasistatic approach, which indicates that the measurements were obtained while the truck was stationary as it slowly moved from one marker to the next. The following forces were transferred from the truck's axles to the structure: front axle (P_1 = 54.0 kN), middle axle (P_2 = 129.0 kN), and rear axle (P_3 = 102.0 kN).

The markings with subsequent numbers *i* have been set along the road at intervals of every 0.675 m, where $i = 0$ located on the axis symmetry of the structure Fig.3[(a)]. The measurement started when i = 7, i.e., when middle axle, P_2 is at distance 4.725 m from the axis of the structure. Then the truck crosses the structure, and the first travel will end once the P_2 reaches i = −3, i.e., when P_2 moves −2.025 m away from the central axis of the structure. Then truck return back without turning until P_2 back to initial starting point, i = 7 by creating a loop. During this successive movement of truck over the bridge, the measurement was taken at bottom of crown of the shell as shown in Figs [3(a–b)].

The initial study report by Ref. [3] presents the results of field tests performed during two phases, namely before and after the pavement on the bridge. The field measurement on the unpaved bridge is considered in this paper.

In the numerical simulation, parametric analysis was conducted to validate the model based on the measured vertical displacement

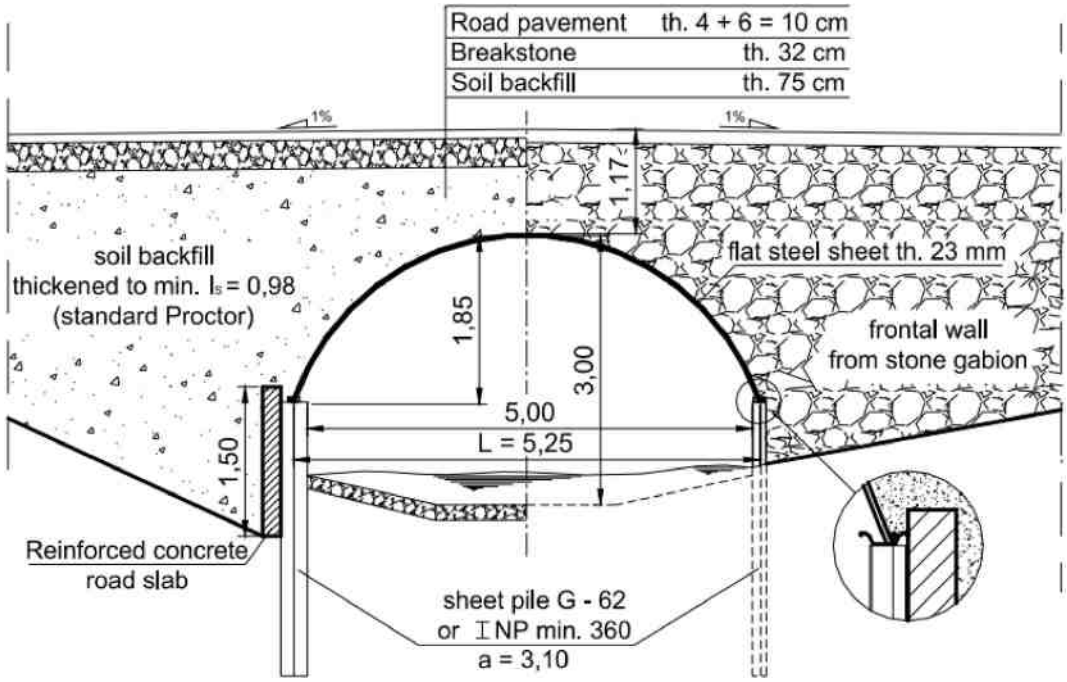

Fig. 2. Cross section of the tested structure [3].

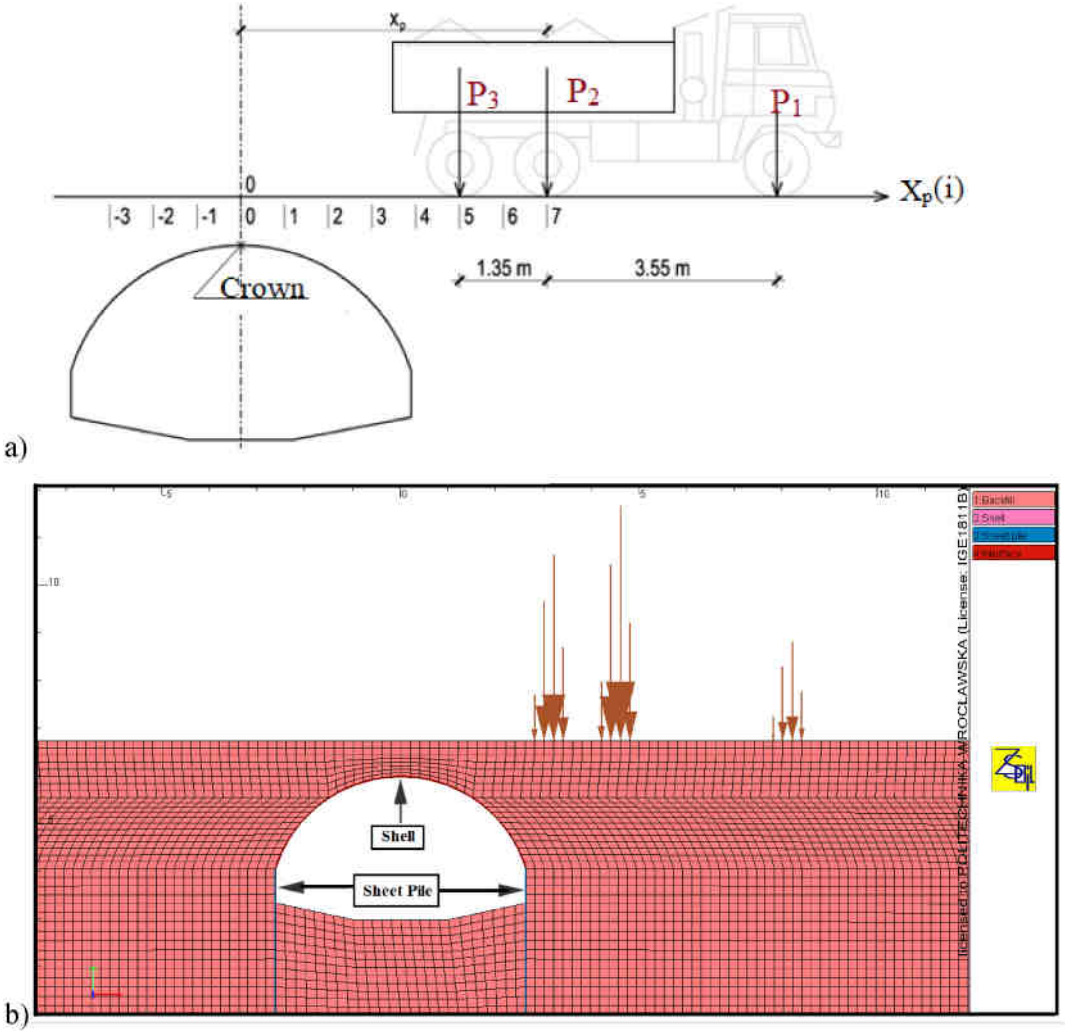

Fig. 3. Loading arrangement, a)for test b) for numerical modelling.

at the crown of the shell. The difference between the measurement and model for absolute maximum vertical displacement is less than ten percent. Thus, successful calibration of the computational model is demonstrated.

2.2. Testing results

On the horizontal axis of Fig. 3[(a)], the position (i number) of the truck as it travels along a designated movement track described (moving along the bridge axis). It's important to note that the measuring cycle on the structure typically commenced when the truck was at position $i = 7$. At this initial position, the sensors indicated a minimum deflection as shown Fig. 3 [(a)]. Subsequently, the truck was driven back in the proper direction and stopped at predetermined positions to facilitate the automatic registration of the measurement results.

In the field test [3], vertical displacements were meticulously measured perpendicular to the steel shell surface, with a particular focus on the crown of the structure. This measurement setup allowed to capture the response of the structure subjected truck load accurately. The results of these measurements, specifically the vertical displacements occurring at the crown.

A distinctive and significant characteristic observed in the field test is the consistent shift of extreme deflections in the direction of the truck's movement, particularly the first drive with reference to the return drive. This shift in extreme deflections is a key finding of the study. Particularly, the deflection extrema are prominently formed under the P_2 (middle) and P_3 (rear) axles when they are positioned over the crown of the shell. This observation indicates that the structural response, specifically the vertical displacements (SeeFig. 4[(a)]), is most pronounced when these axles are in proximity to the crown. Moreover, these extrema align with the positions of specific truck axles further emphasize the direct relationship between the loading configuration and the structural response.

Fig. 4[(b)] displays the curve representing the normal stress in the circumferential direction (σ_x) at the same point, crown of the shell. Similar to the displacement curve, the presence of shift of extreme value of stresses in the direction of the truck's movement.

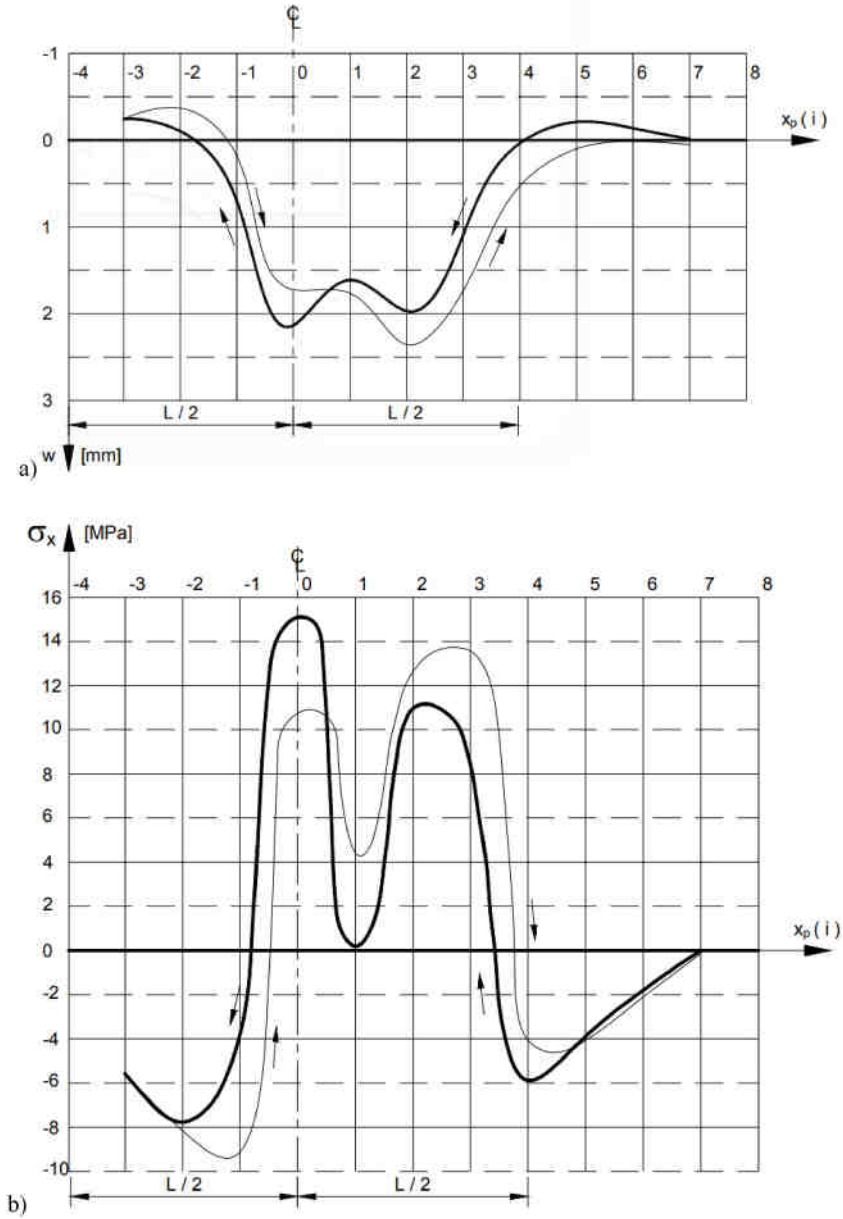

Fig. 4. Results from the field measurement at the crown of the shell a) vertical displacement b) stress [3].

To sum-up, the results obtained from measurement by Ref. [3], reveal an interesting behavior in the structural response of the soil steel composite structure under vehicular loading conditions. Specifically, the curves corresponding to the displacements and stress (See Fig. 4[4(a–b)]) exhibit hysteresis loops, which indicate a unique and significant characteristic of the structural response.

Hysteresis loops in structural response curves are of significant interest and importance in structural engineering and mechanics. They indicate that the response of the structure is history-dependent, meaning it not only depends on the current loading but also on its previous loading history. This behavior can be attributed to various factors, including material behavior, nonlinearities, and energy dissipation within the structure.

3. Formulation of computational model

The ZSoil software programme [39], based on FEM, was used for the numerical analysis of the structure of the behaviour of SSCSs subjected to quasi-static moving load. The structure was modeled as a 2D object in plane strain using beam elements for the shell structure and sheet piles while solid elements for backfill soil. The bottom boundary was fixed in all directions, while the vertical

boundaries were restricted against horizontal displacements. In the numerical calculation, a plain strain analysis was assumed. For backfill soil, elasto-plastic constitutive model with the Mohr-Coulomb yield criterion is assumed. The unassociated plastic flow rule is described by a ZSoil user manual used to determined dilatancy angle based on Eq (1) [39]:

$$\psi = max\ (0.1\varphi, \varphi - 25^{\circ}) \tag{1}$$

where φ the internal angle of friction and ψ is the dilatancy angle.

The interface between shell and backing soil is generated in the model. A one-sided contact was assumed at the interface, i.e., separation of the backfill material from the shell is permitted if the shell moves away from the backfill material and subsequent contact renewal is permitted if the backfill and shell get closer again. The Coulomb condition was used to describe the behaviour of the assumed interface. A non-associated plastic flow rule was used to govern a plastic slip, with the dilation angle set to $\psi = 0$. The Coulomb condition governs the value of maximum tangential stress in contact elements based on Eq (2):

$$|\tau_f| \leq a + \sigma\ tan\ \delta \tag{2}$$

Where adhesion a = 0, the angle of friction $\delta = 0.6\ \varphi$ and $\varphi = 34^{\circ}$ is the internal friction angle of the backfill material adjacent to the interface. The dilation angle ψ, was assumed as zero. Elastic deformation moduli (normal and tangential stiffness) for interface elements were determined according to the Zsoil user manual [39] as follows:

$$K_n \approx K_t = \frac{E}{h} \tag{3}$$

Where E is its modulus of adjacent material, that is, the filling soil, and h is the depth of the very thin weak layer. Based on Eq (3), the value of normal and tangential stiffness adopted in the calculation was 1.5×10^7 kN/m.

The parameters of backfill soil in a dense compaction state, i.e., density index $I_D = 0.8$ considered in the model. The shell and sheet pile are modeled as beam elements and linear elastic constitutive relations were assumed for both materials. Sheet piles of type G-62 were assumed and positioned at a distance of 3.1 m. The parameters for the material used in the numerical computations are shown in Table 1. To avoid premature termination of the calculation due to soil failure under moving load and to ensure the numerical stability of the model, the value of cohesion was increased.

As this study aims to investigate the effect of spacing, six different models of different distances between shells are created. Furthermore, a single-shell structure reference model is considered for calibration purposes. All the models mentioned, in terms of their geometry, are presented in Figs [5(a – g)].

The first model was prepared as a single shell, that is, without lateral shells, as shown in Fig [5(g)]. The displacement and stress from this model are used as a reference to understand the effect of the lateral shells on the central one at a different distance. The quasi-static approach of moving truck was simulated as presented in previous works [14,19,24,25,40].

3.1. Parametric analysis

A steel shell with a span of 5.25 m and a depth of 0.75 m cover was examined together with two lateral shells with five different spacings (see Fig. 5). These spacings are 0.0, 0.6, 2.625, 5.25, 10.5, and 15.75 m, corresponding to a spacing-to-span ratio (S/D) of 0.0, 0.114, 0.5, 1.0, 2.0, and 3.0, respectively. In the third model, 0.6 m of space was provided between the shells. This distance was the minimum distance recommended by Ref. [41] for short-span structures based on the type of profile and the span of the structure to be considered. The initial stress by the dead weight load was the first phase of the simulation. The simulation was then continued by applying the load exerted by the truck at its starting position. The position of the truck load is labelled by the variable X. When X = 0 the truck load is at the center of the structure (see Fig. 6). Three hundred successive load locations were carried out during the truck movement between extreme positions (X = −30.0 m; X = +30.0 m). In the simulation, it was assumed that the forces of the truck axis were distributed on the width of the track in the transverse direction and at a distance of 0.5 m along the bridge, similar to the assumption proposed by Ref. [24]. The reduced load P were calculated based on Eq (4) [42].

$$q = \frac{P}{b} \tag{4}$$

Table 1
The material parameters used in the computations.

Steel Sheet		Steel pile	Backfill soil
Young's modulus	205 GPa	205 GPa	150 MPa
Poisson ratio	0.3	0.3	0.25
Moment of Inertia	1.01×10^{-6} m^4/m	9.833×10^{-6} m^4/m	–
Sectional area	1.91×10^{-2} m^2/m	2.07×10^{-3} m^2	–
Unit weight	78.6 kN/m^3	78.6 kN/m^3	19 kN/m^3
Cohesion	–	–	10 kPa
Friction angle	–	–	34°
Dilatancy angle	–	–	9°

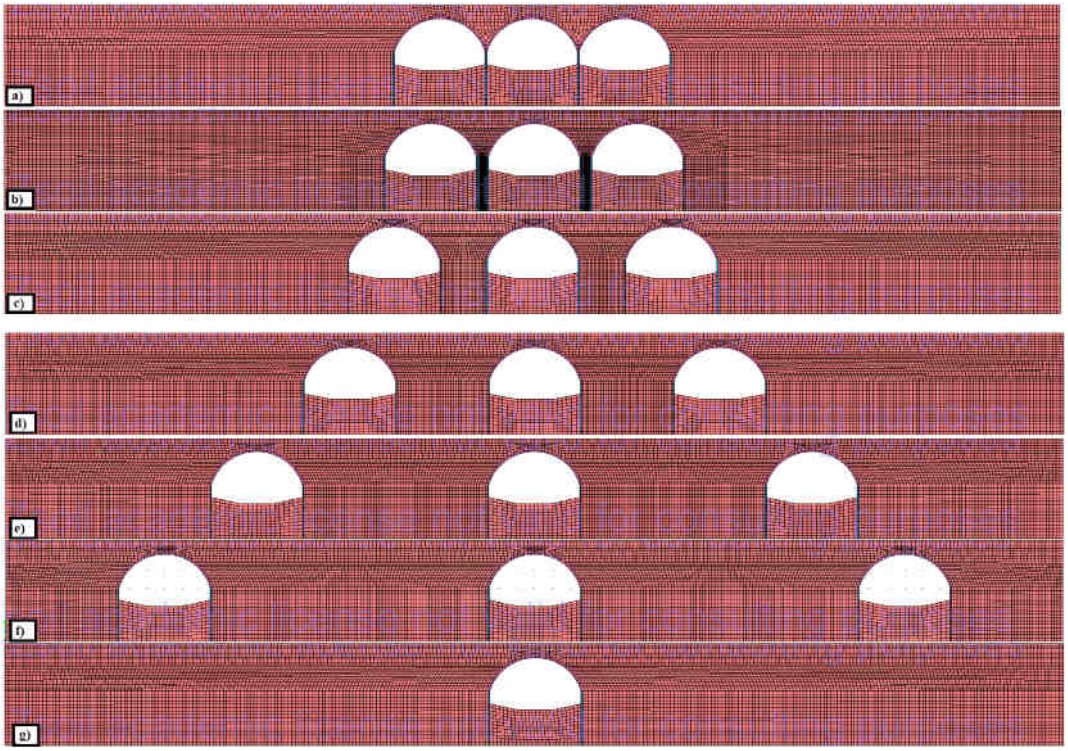

Fig. 5. Geometry of numerical models: a) no space between the shells b) 0.6 m spacing c) half of the span spacing d) spacing equal to span e) twice of span spacing f) three-time span spacing g) infinite spacing or reference bridge.

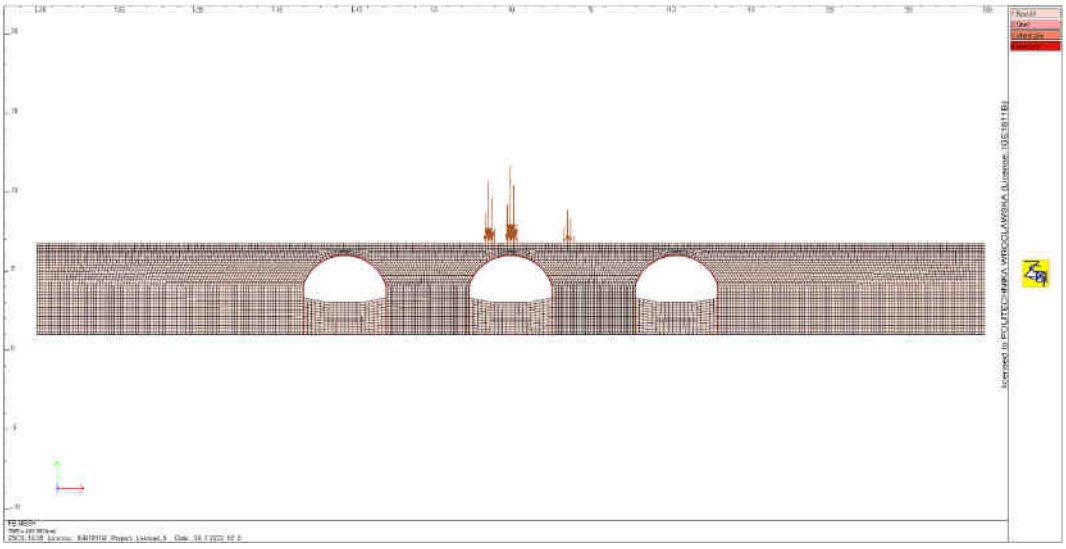

Fig. 6. Equivalent nodal forces from truck loads.

where P is the value of the force transferred from the.

axle load (($P_1 = 54.0$ kN, $P_2 = 129.0$ kN, and $P_3 = 102.0$ kN)) and

b' the reduced width of the impact of truck.

Because of their 3D distribution, soil stresses decrease as depth increases. creating a similar effect in 2D is impossible. As a result, the impact width b' was calculated by proper calibration based on field measurement displacement. Accordingly, the reduced width b' = 1.8 m and the corresponding distributed loads are $q_1 = 60.0$ kN/m, $q_2 = 143.3$ kN/m, and $q_3 = 113.3$ kN/m. Similar assumptions were considered by Refs. [11,20].

The numerical analysis assumed four passes of the truck over the bridge, that is, two complete load cycles consisting of "forward" and "back" travel. The live load from the truck is added to the model after the soil fill has been laid, but before the road foundation and asphalt surface are laid. That means that in this model, the effect of road foundation and pavement was not taken into account. Based on the position of the lateral shells, seven different models were developed, including the reference model, Fig. 5[(g)]. The first model was prepared without lateral shells. The result of the simulation is described in the next section.

4. Simulation results

4.1. Validation of numerical model

Given the challenge of conducting experiments on multi-span SSCS with varying shell spacing, a decision has been made to employ field measurements on a single span SSCS as outlined in Section 2. The numerical model has been validated using thus field tests conducted on this particular structure subjected to quasi-static moving loads.

The measured displacement and stress at the bottom of the shell crown (at reference crown) in Fig [2(a)] sets the basis for the validation of the numerical model. Taking into account these measured displacements, a parametric analysis is conducted to calibrate the input parameters like modulus of elasticity, cohesion, friction angle, and interface stiffness, i.e., both normal and tangential. The main objective of this calibration is to fit the absolute maximum displacement and stresses during the first passage. Accordingly, the calibration of the FE model is successfully carried out using the results of measured displacement and stress, as shown in Fig (7) and Fig (8), respectively.

The absolute maximum vertical displacement observed in the field test at the crown of the shell is approximately 2.4 mm [3] as shown Fig[4(a)]. While numerical simulation predicts an absolute maximum displacement of approximately 2.54 mm. These results demonstrate a close agreement between the field test and numerical simulation, with the simulation slightly overestimating the maximum vertical displacement. Nevertheless, it is important to note that the difference is less than 6 %. Furthermore, the finding from both the field test and numerical pertains to a consistent shift in the location of the maximum vertical displacement, occurring in the direction of the truck's movement. This phenomenon provides a clear indication that the structural response is asymmetrical and influenced by the position of the truck's axle during its passage over the structure. This highlights the effects of loading position on flexible soil steel composite structures.

The values of stress are underestimated but the course of the chart is in good agreement with the experimental one. This suggests that while the absolute values may differ, the trends and patterns of stress distribution are captured effectively by the numerical model. Similar to the vertical displacement, a significant finding in both the field test and numerical simulation is the consistent shift of extreme stress values in the direction of truck movement for consecutive truck passes. Thus, the results obtained numerically exhibit the same tendency as those identified experimentally.

In conclusion, the comparative analysis of field test and numerical simulation results for the vertical displacement and stress at the crown of the shell demonstrates a good level of agreement, providing validation for our numerical model.

4.2. Numerical results

The Selected vertical and horizontal displacement, as well as the stress, σ_x results obtained from the six different models of the SSCSs are shown in Figs 9–11. The graphs show the change in shell displacements and stress caused by the truck passage and the position of the lateral shells. The results of the displacements and stress at the crown of the central shell are presented. The graphs illustrate changes in central shell displacement produced by the trucks' initial and returning travels, as well as the position of the lateral shells. On the basis of these results, an effect of the position of the lateral shells on the deformation of the central shell is observed (see Fig. 12).

The stress at the crown of the central shell, presented here as a numerical simulation result, was calculated based on Eq. (5):

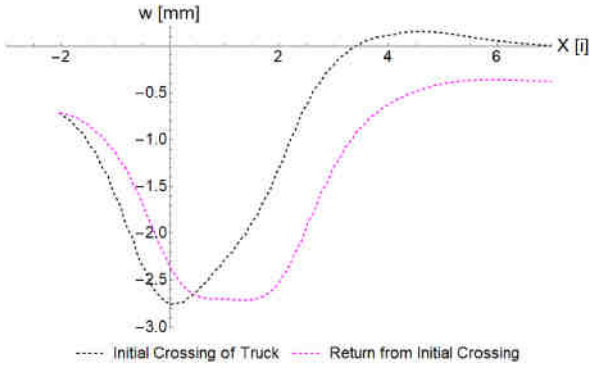

Fig. 7. Vertical displacement curve at the crown of the shell during consecutive truck crossings.

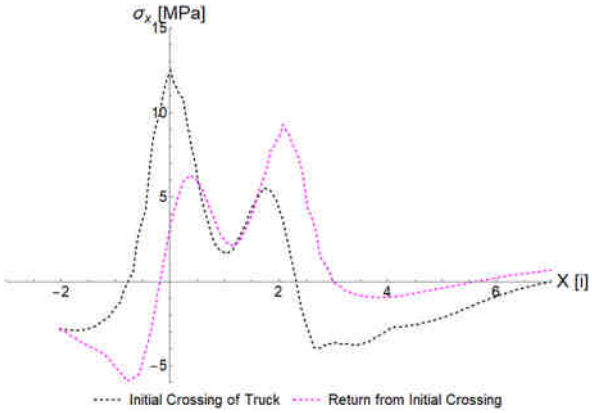

Fig. 8. Circumferential stress at the crown of the shell during consecutive truck crossings.

$$\sigma_x = \frac{(N - N_0)}{A} + \frac{(M - M_0)}{I} \cdot \frac{h}{2} \tag{5}$$

where N, M stands for the axial force and the bending moment, respectively, and N_0 and M_0 are the values of the axial force and moment for the calculated structure at the start of the test, I and A are moment of inertia and the cross section area respectively. while h is the thickness of the steel shell.

Under the scope of this numerical modeling, we have obtained critical results pertaining to the vertical and horizontal displacements, as well as stress distributions, at the crown of a shell of soil-steel composite structure. Our investigation centered on understanding how the bridge responds as a truck cross it, both in backward and forward movements in quasi-static manner, without any turning. To create a robust modeling scenario, the truck completed four crossings in total by traversing the bridge twice in each direction. The visual representations in Figs 9–11 illustrate these crossings, with the initial crossing of the truck from x = L to x = -L highlighted in blue, and the return from x = -L to x = L marked with dashed blue lines. Similarly, the second crossing from x = L to x = -L is depicted in red, and the return from x = -L to x = L is denoted with dashed red lines.

Notably, our analysis reveals that the values of the displacements and stress change as the direction of movement changes. These variations in displacement and stress are critical to understanding the bridge's dynamic behavior under the influence of the truck's movements. Furthermore, our results consistently show the creation of hysteresis loops, indicating that the bridge's response is not only dependent on the current loading but also on the previous loading history. The presence of hysteresis loops in the results highlights the importance of considering the bridge's past loading conditions when assessing its response. These findings represent essential contributions to bridge design and analysis, shedding light on the complex behavior of soil-steel composite structure under repetitive truck crossings.

Also As illustrated in Figs 9–11, the outcomes of our numerical simulations reveal a pronounced sensitivity to not only the direction of the movement of truck but also the position of the lateral shells. The results exhibit significant variations, both in terms of quantitative values and qualitative behavior, depending on the specific positioning of the lateral shells, the direction of the load, and the interaction with the structure. These findings highlight the complexity of the interactions within the shell of the multi-span soil-steel composite structure under different loading conditions. The position of the lateral shells plays a crucial role in distributing and transmitting the load across the bridge's span. Depending on the lateral shell configuration and load direction, the central shell's response can range from subtle variations in displacements and stress to more pronounced changes in structural behavior.

5. Discussion

A significant phenomenon observed in our simulations is the considerable uplift of the shell during successive truck crossings when the truck initially starts moving over the bridge. This uplift phenomenon is more pronounced when the lateral shells are in close proximity to the central shell as depicted in Figs [9(a–g)], resulting in an upward tilt of the shell. As the truck advances toward the crown of the shell, this uplift of the shell gradually decreases, and the vertical displacement reaches its maximum when the truck aligns with the crown during consecutive load cycles, consistent across all simulations. Each subsequent load cycle, or truck pass, induces irreversible changes in the shell's behavior, particularly when the lateral shells exert lateral pressure on the central shell due to their proximity. This lateral pressure significantly impacts the structure's load-bearing capacity.

Notably, our simulations consistently yield closed hysteresis loops in the vertical displacement graphs for all scenarios, indicating the bridge's ability to maintain a consistent behavior under cyclic loading conditions. This alignment between our simulated results and field measurements, as observed in a single-span shell by Ref. [3], underscores the accuracy of our modeling approach and offers valuable insights into the dynamic response and stability of the soil-steel composite bridge.

Based on the analysis conducted, the maximum vertical displacement, *w,* that occurred in the central steel frame is within a range of −5.99 to 4.084 mm Fig [9(b)] as compared to the in situ measurement without lateral frame, which ranges of −2.5 to 0.5 mm [3].

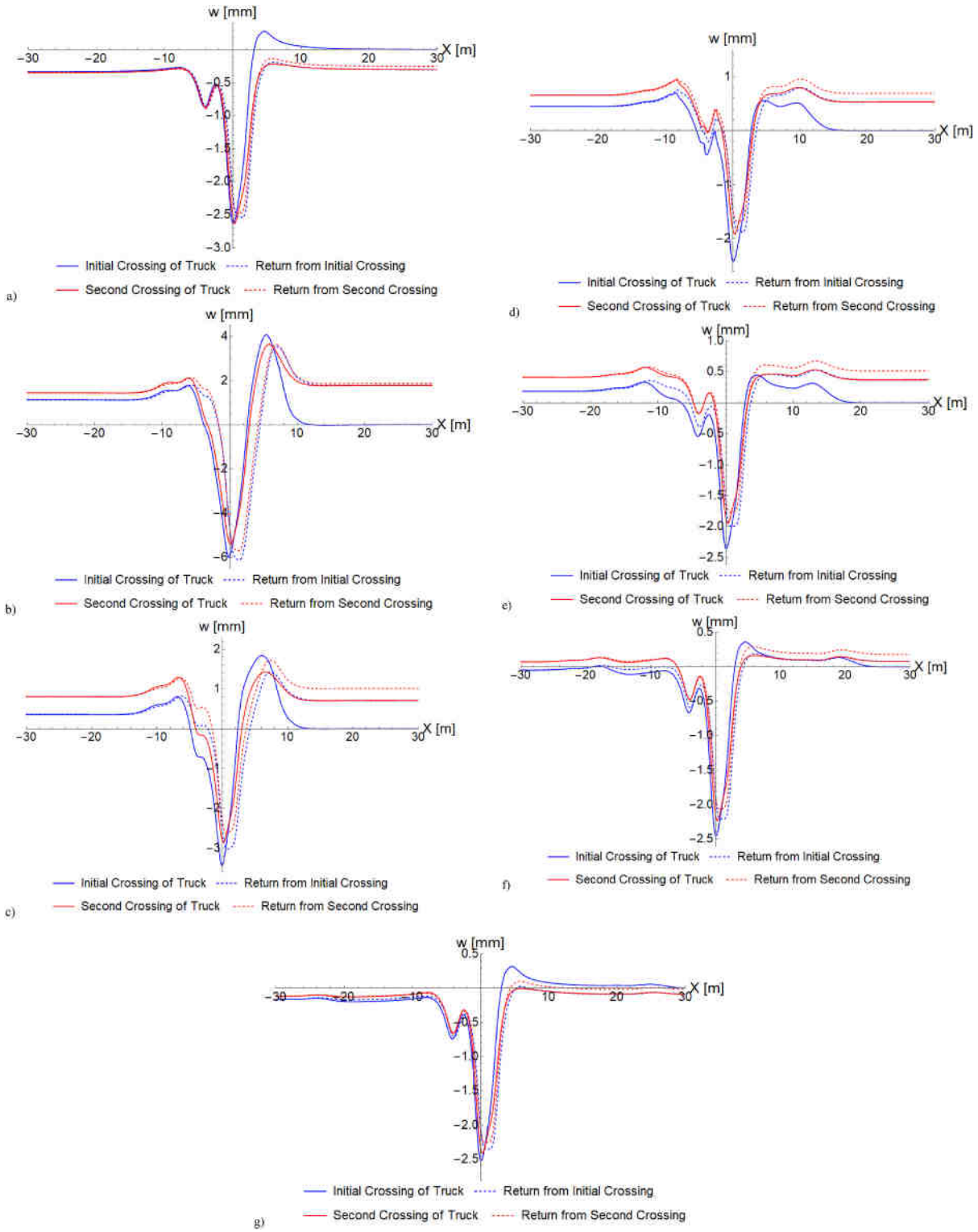

Fig. 9. Vertical displacement at the crown of the central shell during consecutive truck crossings: (a) reference (b) central shell at 0.0 m distance from lateral shell (c) at 0.6 m (d) at 2.625 m (e) at 5.25 m (f) at 10.5 m (g) at 15.75 m.

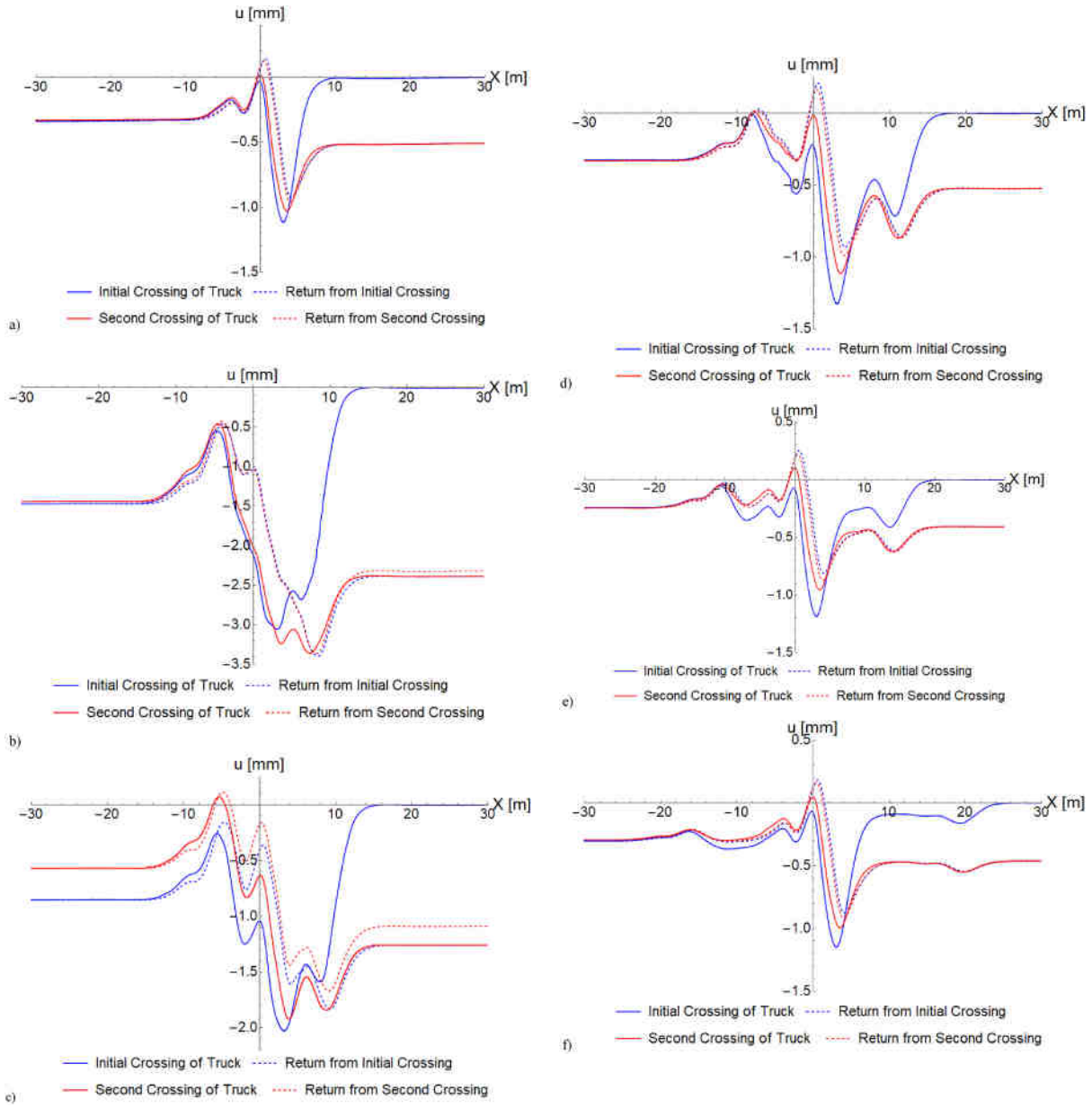

Fig. 10. Horizontal displacement in the central shell crown during consecutive truck crossings: (a) reference, (b) central shell at 0.0 m distance of from the lateral shell (c) at 0.6 m (d) at 2.625 m (e) at 5.25 m (f) at 10.5 m (g) at 15.75 m.

Maximum vertical displacement was observed during the first truck travel when the lateral shells were placed at a distance of 0.0 m from the enteral shell. However, significant reductions have been observed when the lateral cover was placed at a distance of 0.6 m (ranging from −3.452 to 1.842 mm). From these two simulation results, it can be concluded that providing a spacing of around 10 % of the span of the structure has a significant impact on the reduction of vertical displacement. When the lateral supports are placed half of the span of the bridge (2.625 m) from the central support, the vertical displacement at the crown of the central support was almost similar to the reference support (no lateral shells), as shown in Fig [9(a)] and Fig [9(d)]. As shown in Figs [9(e–g)], the change in vertical displacement was almost constant.

The reduction in deformation as span spacing increases can be attributed to a variety of factors. For instance, backfill plays a crucial role in providing support, stability, and load distribution to this particular type of structure. Furthermore, it provides lateral support to the shell of SSCS, aiding in the resistance of the lateral forces and reducing deformation in the shell induced by vehicular loads. Consequently, a substantial portion of the load-bearing capacity and stiffness of SSCS is achieved through interaction with the backfill material. This indicates that as the spacing increases, the shell receives more support from the backfill, leading to increased stiffness of

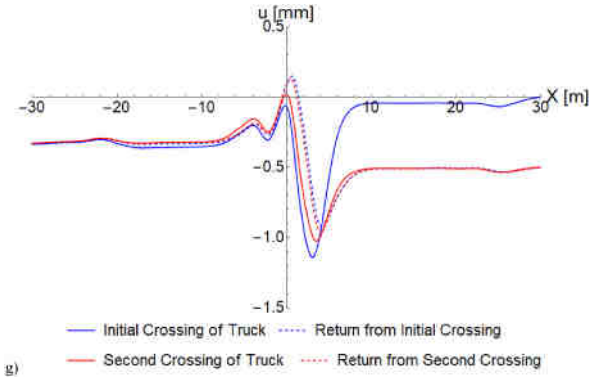

Fig. 10. (*continued*).

the composite structure and a more uniform distribution of the truck load across the spans. Consequently, this could result in reduced deflection at the central shell.

In all models Figs [9(a–8g)], the maximum vertical displacement occurred during the first passage of the truck, and when the truck moves away from the structure, the deflection decreased but did not return to zero, i.e., the residual displacements remained. A similar phenomenon was observed in earlier studies [16,32]. The extreme vertical deflection shift is observed in the direction of truck movement. This shift was basically due to the difference in the magnitude of the axle loads. The deflection extrema are formed under the P_2 (middle) and P_3 (rear) axles when they are in the crown of the shell. This means that the extreme deflections for the backward movement and forward movement of the truck are not at the same position as observed in Figs [9(a–g)]. A similar result was observed in the work of [3,24]. Understanding these characteristics is crucial for assessing the structural integrity of the shell under loads, such as those imposed by vehicular traffic. It provides insights into the points of maximum stress and deformation, which are essential considerations for structural design and analysis.

In contrast to vertical displacement, the maximum horizontal displacement in the range of −0.46 to −3.39 mm was observed during the second travel, i.e., the return of the truck from the first trip (the blue dashed line in Fig [10(b)]. However, it was observed when the lateral shells were placed at a 0.00 m distance from the central shell, as in the case of vertical displacement. Once the lateral shells were placed at 0.6 m from the central shell, the displacement decreased to a range of (0.1 to – 2.03 mm) Fig [10(c)]. At 2.625 m (half of the span of the considered bridge), the displacement decreased, (0.2 to −1.33 mm). Compared to the reference, the increment is only 21 %. Like the vertical displacement, the effect of lateral shells is not much significant when they are placed at a distance greater than half of the span of the structure. Consequently, the horizontal (absolute) displacements at spacings of 5.25, 10.5, and 15.75 m are 1.19, 1.15, and 1.14 mm, respectively.

In other words, when the ratio between the spacing (S) and the span (D) of the structure (S/D) $\geq$ 0.5, the effect of the lateral shell on the displacements of the central shell is negligible, as shown in Figs [12(a –b)]. This indicates that the lateral shells have no such significant influence on the vertical displacement of the central shell under live load when they are spaced at a distance equal to or greater than half the span of the structure.

However, in contrast to vertical displacement, the residual displacement was extensive in horizontal displacement. In all models Figs [10(a–g)] except the model without spacing, the absolute maximum horizontal displacement occurred during the first passage of the truck, and when the truck left the structure, the displacement decreased but did not return to zero, that is, the residual displacements remained. Compared to vertical displacement, residual displacements are very large. The extreme maxima are shifted in the direction of the truck movement as a vertical displacement.

In both vertical and horizontal displacements, there is a significant difference in the displacements registered during the truck's passage over the structure, depending on the direction of the crossing. This phenomenon, known as the hysteresis effect, had already been discovered in other soil-steel composite structure in the work [14,16,21,32,33].

The results of the circumferential stress σ_x for models are presented on Figs [11(a–g)]. The maximum value of circumferential stress σ_x was observed when the lateral shell is placed at 0.0 m, as presented in Fig [11(b)]. From the graphs, the stress ranges from −12.607 to 20.855 MPa. The magnitude of stress is significantly increased compared to the in situ stress test [3], which was (−10.0 to 15.0 MPa).

Similarly, to displacements, a significant reduction in stress (absolute) was observed when the lateral shells were placed at a spacing greater than half the span of the structure. The values of the extreme maxima (absolute) at 2.625, 5,24, 10.5, and 15.75 m spacing are 11.47, 10.51, 10.79, and 10.87 MPa, respectively, as shown in Fig(13). The finding of [38] also concluded that in two span SSCS, stress significantly decreases as the spacing increases.

The relation between stress in the crown of the central shell and spacing (S) is shown in Fig(13). From this figure, it can be clearly seen that the narrow spacing between the layers has a considerable effect on the induced circumferential stress (σ_x), since the adjacent and unloaded layer provides supports with lower stiffness to the side of the loaded layer. A similar conclusion was formulated by Ref. [43].

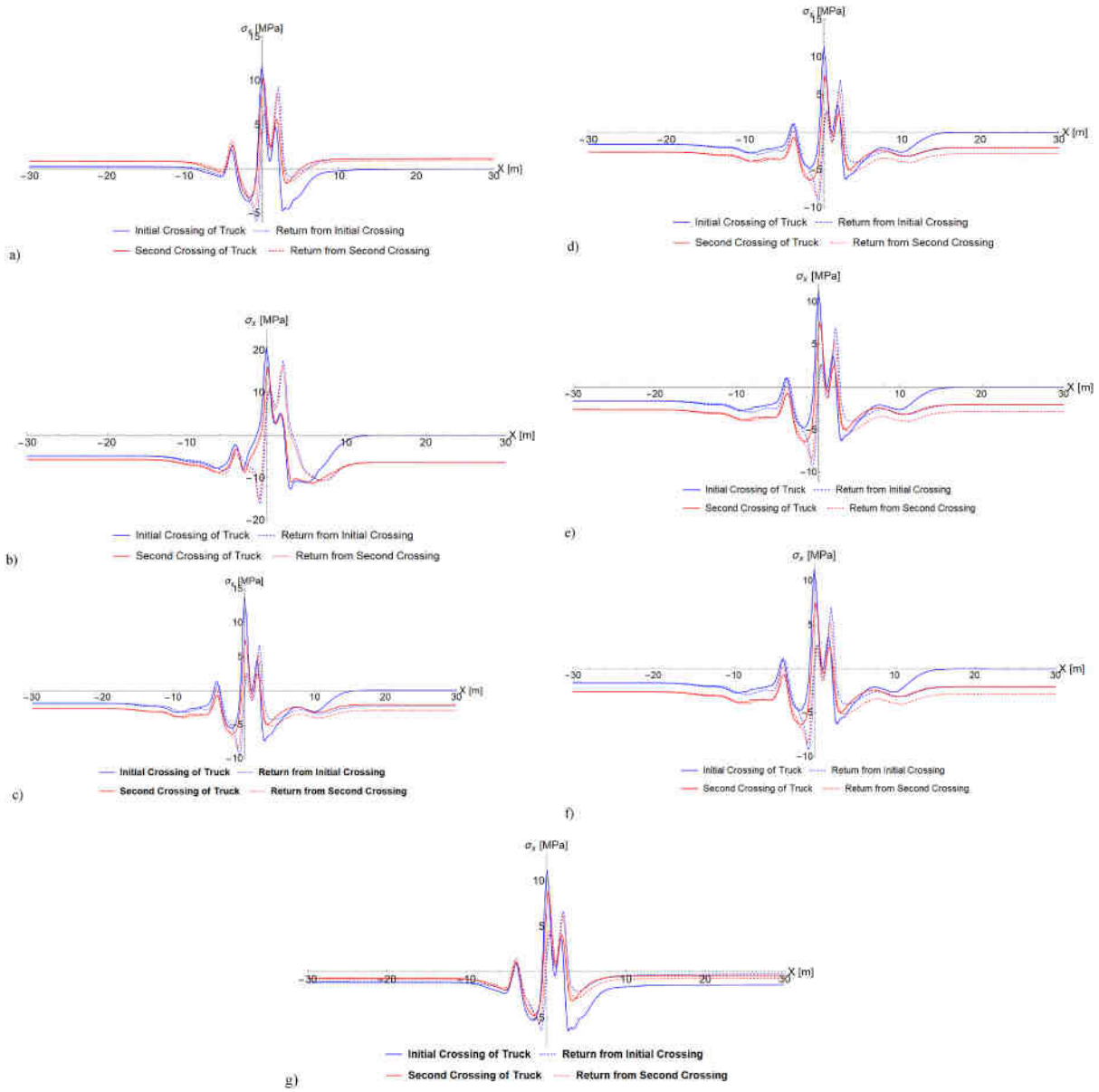

Fig. 11. Stress in the crown of the central shell during consecutive truck crossings: (a) reference (b) central shell at 0.0 m distance of from the lateral shell (c) at 0.6 m (d) at 2.625 m (e) at 5.25 m (f) at 10.5 m (g) at 15.75 m.

6. Summary and conclusions

The effect of lateral shells at different positions on the mechanical behaviour of the central shell under live load was investigated numerically. The constitutive model for the backfill soil was elastic-perfectly plastic and linear elastic for the shell as well as the sheet piles. The plastic slip along the soil-steel contact interface was described in terms of the Coulomb condition with the dilation angle value set to $\psi = 0$. The main conclusions drawn from the numerical simulations conducted are as follows:

- Vertical and horizontal displacement increase significantly when the S/D ratio is 0.5. Providing 0.6 m spacing, which is almost 10 % of the span of the structure, the displacements are substantially decreased almost by 50 % compared to the field test.
- Maximum stress in the central shell is observed when the lateral shells are placed at a 0.0 m distance. Similarly, to displacements, the stresses at the crown of the central shell are decreased by 35 % by providing 0.6 m spacing.
- Extreme displacement and stress values change in the direction of truck movement. These characteristics is crucial for assessing the structural integrity of the shell under different loading conditions, such as those imposed by vehicular traffic. It provides insights into the points of maximum stress and deformation, which are essential considerations for structural design and analysis.

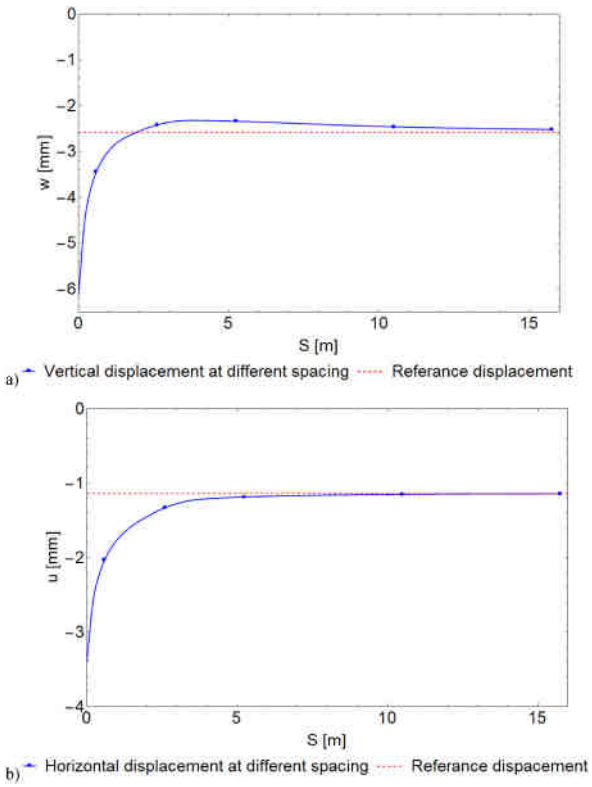

Fig. 12. Displacements at the Crown of the Central Shell vs. Shell Spacing During Truck Crossings (a) Vertical and (b) Horizontal.

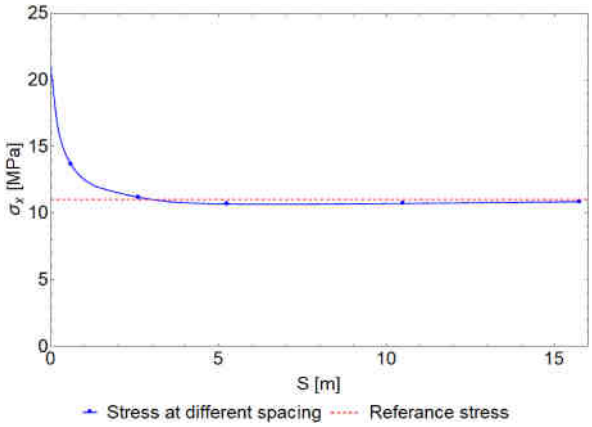

Fig. 13. Stress at the Crown of the Central Shell vs. Shell Spacing During Truck Crossings.

- The effect of non-zero residual displacements and stress, which remain in the structure after consecutive load cycles, is clearly visible and more evident in horizontal displacement compared to vertical displacements. The residual stress decreased as the S/D ratio decreased.
- The effect of the position of the lateral shells on the displacements and stress of the central shell is not significant when $S/D > 0.5$.
- Closely spaced conduits are considerably affected by each other because their support is stiffer than that of their other counterparts.
- The load carrying capacity of the multi-span SSCSs increases with the increase in spacing between the adjacent shells. It is recognized that the interaction between closely spaced SSCSs is affected by the spacing between them. However, for practical purposes, considering the minimum spacing based on factors such as the size and shape of the shell, as well as the depth of cover in the soil, is essential.

Funding

This research did not receive external funding.

Data availability statement

Data will be made available on request.

CRediT authorship contribution statement

Alemu Mosisa Legese: Writing – review & editing, Writing – original draft, Validation, Software, Methodology, Investigation, Formal analysis, Conceptualization. **Adrian Różański:** Writing – review & editing, Supervision, Methodology, Conceptualization. **Maciej Sobótka:** Writing – review & editing, Supervision, Methodology, Conceptualization.

Declaration of competing interest

The authors declare that they have no known competing financial interests or personal relationships that could have appeared to influence the work reported in this paper.

References

[1] B. Bakht, Evolution of the design methods for soil–metal structures in Canada, in: Arch. Inst. Civ. Eng. Eur. Conf. Buried Flex. Steel Struct. Pol., Politechnika Poznańska, Wydawnictwo Politechniki Poznańskiej, 2007, pp. 7–23.
[2] E. Flener, R. Karoumi, Evaluation of the dynamic response of a soil-steel composite railway bridge, in: Buried Flex. Struct., Politechnika Poznańska, Wydawnictwo Politechniki Poznańskiej, 2012, pp. 55–64.
[3] G. Antoniszyn, C. Machelski, B. Michalski, Live load effects on a soil-steel bridge founded on elastic supports, Stud. Geotech. Mech. 28 (2006) 65–82.
[4] Gonzalo Ramos Schneider, Lars Pettersson, Soil Steel Composite Bridges an International Survey of Full Scale Tests and Comparison with the Pettersson-Sundquist Design Method, 2014.
[5] ViaCon Poland, Catalogues English. https://viacon.pl/en/download, 2022. (Accessed 11 February 2022).
[6] D. Beben, Soil-Steel Bridges; Design, Maintenance and Durability, Springer Nature, Opole, Poland, 2020, https://doi.org/10.1007/978-3-030-34788-8.
[7] Y.F. Girges, Three-dimensional Analysis of Composite Soil-Steel Structures, University of Windsor, 1993.
[8] C. Zhang, M. Su, C. Zhu, M. Wang, Bearing performance of high-strength bolted corrugated steel longitudinal seams, J. Constr. Steel Res. 198 (2022), 107538.
[9] T. Maleska, J. Nowacka, D. Beben, Application of EPS geofoam to a soil–steel bridge to reduce seismic excitations, Geosci. 9 (2019), https://doi.org/10.3390/geosciences9100448.
[10] P. Mellat, A. Andersson, L. Pettersson, R. Karoumi, Dynamic behaviour of a short span soil–steel composite bridge for high-speed railways – field measurements and FE-analysis, Eng. Struct. 69 (2014) 49–61, https://doi.org/10.1016/J.ENGSTRUCT.2014.03.004.
[11] A. Sanaeiha, M. Rahimian, M.S. Marefat, Field test of a large-span soil–steel bridge stiffened by concrete rings during backfilling, J. Bridg. Eng. 22 (2017), 06017002, https://doi.org/10.1061/(asce)be.1943-5592.0001102.
[12] L. Pettersson, Full Scale Tests and Structural Evaluation of Soil Steel Flexible Culverts with Low Height of Cover, KTH Royal Institute of Technology, 2007. http://digilib.unila.ac.id/11478/16/16.BABII.pdf.
[13] L. Pettersson, E.B. Flener, H. Sundquist, Design of soil–steel composite bridges, Struct. Eng. Int. 25 (2015) 159–172, https://doi.org/10.2749/101686614x14043795570499.
[14] M. Sobótka, D. Łydżba, Live load effect in soil-steel flexible culvert: role of apparent cohesion of backfill, Eur. J. Environ. Civ. Eng. 8189 (2019), https://doi.org/10.1080/19648189.2019.1670264.
[15] E. Ołdakowska, Flexible engineering structures from the corrugated metal sheets - comparison of costs of solutions used in the road building, IOP Conf. Ser. Mater. Sci. Eng. 269 (2017), https://doi.org/10.1088/1757-899X/269/1/012025.
[16] E.B. Flener, Response of long-span box type soil-steel composite structures during ultimate loading tests, J. Bridg. Eng. 14 (2009) 496–506, https://doi.org/10.1061/(asce)be.1943-5592.0000031.
[17] M. Esmaeili, J.A. Zakeri, P.H. Abdulrazagh, Minimum depth of soil cover above long-span soil-steel railway bridges, Int. J. Adv. Struct. Eng. 5 (2013) 1–17, https://doi.org/10.1186/2008-6695-5-7.
[18] A. Wadi, A Comparison between the Pettersson-Sundquist AMER H vol. 2012, H . WADI Master of Science Thesis Stockholm, Sweden, 2020.
[19] C. Machelski, M. Sobótka, S. Grosel, Displacements of shell in soil-steel bridge subjected to moving load: determination using strain gauge measurements and numerical simulation, Stud. Geotech. Mech. 44 (2022).
[20] T. Maleska, D. Beben, The impact of backfill quality on soil-steel composite bridge response under seismic excitation, IOP Conf. Ser. Mater. Sci. Eng. 419 (2018), https://doi.org/10.1088/1757-899X/419/1/012040.
[21] E. Bayoglu Flener, Testing the response of box-type soil-steel structures under static service loads, J. Bridg. Eng. 15 (2010) 90–97, https://doi.org/10.1061/(ASCE)BE.1943-5592.000004.
[22] J. Nowacka, D. Beben, T. Maleska, Analysis of soil-steel bridge with EPS geofoam under static loads, in: Bridg. Maintenance, Safety, Manag. Life-Cycle Sustain. Innov., CRC Press, 2021, pp. 1816–1823.
[23] M. Sobótka, D. Łydzba, Shape optimization of soil-steel structure by simulated annealing, Procedia Eng. 91 (2014) 304–309, https://doi.org/10.1016/j.proeng.2014.12.065.
[24] M. Sobótka, Numerical simulation of hysteretic live load effect in a soil-steel bridge, Stud. Geotech. Mech. 36 (2014) 104–110, https://doi.org/10.2478/sgem-2014-0012.
[25] M. Sobótka, C. Machelski, Hysteretic live load effect in soil-steel structure, Eng. Trans. 64 (2016) 493–499.
[26] E. Bayoğlu Flener, R. Karoumi, Dynamic testing of a soil–steel composite railway bridge, Eng. Struct. 31 (2009) 2803–2811, https://doi.org/10.1016/J.ENGSTRUCT.2009.07.028.
[27] D. Beben, Experimental study on the dynamic impacts of service train loads on a corrugated steel plate culvert, J. Bridg. Eng. 18 (2013) 339–346, https://doi.org/10.1061/(ASCE)BE.1943-5592.0000395.
[28] A. Mahgoub, H. El Naggar, in: Assessment of the Seismic Provisions of the CHBDC for CSP Culverts, Int. Conf. GeoOttawa, Geo Ottawa, Nova Scotia, Canada, 2017, pp. 1–4.
[29] T. Maleska, D. Beben, Behaviour of corrugated steel plate bridge with high soil cover under seismic excitation, MATEC Web. Conf. 174 (2018), https://doi.org/10.1051/matecconf/201817404003.

[30] C. Regier, N.A. Hoult, I.D. Moore, Laboratory study on the behavior of a horizontal-ellipse culvert during service and ultimate load testing, J. Bridg. Eng. 22 (2017), 4016131.
[31] R.W.I. Brachman, I.D. Moore, A.C. Mak, Ultimate limit state of deep-corrugated large-span box culvert, Transp. Res. Rec. 2201 (2010) 55–61, https://doi.org/10.3141/2201-07.
[32] T.M. Elshimi, Three-dimensional Nonlinear Analysis of Deep-Corrugated Steel Culverts, 2011.
[33] K. Embaby, M.H. El Naggar, M. El-Sharnouby, Ultimate capacity of large-span soil-steel structures, Tunn. Undergr. Sp. Technol. 132 (2023), 104887.
[34] A. Wadi, L. Pettersson, R. Karoumi, On predicting the ultimate capacity of a large-span soil–steel composite bridge, Int. J. Geosynth. Gr. Eng. 6 (2020) 1–13, https://doi.org/10.1007/s40891-020-00232-z.
[35] X. Bao, X. Wu, J. Shen, S. Wu, X. Chen, H. Cui, Performance analysis of multiple steel corrugated pipe arch culvert under construction and periodic vehicle load, Appl. Sci. 13 (2023) 9441, https://doi.org/10.3390/app13169441.
[36] Y. Sawamura, K. Kishida, M. Kimura, Centrifuge model test and FEM analysis of dynamic interactive behavior between embankments and installed culverts in multiarch culvert embankments, Int. J. GeoMech. 15 (2015), 4014050, https://doi.org/10.1061/(ASCE)GM.1943-5622.0000361.
[37] J. Hwang, M. Kikumoto, K. Kishida, M. Kimura, Dynamic stability of multi-arch culvert tunnel using 3-D FEM, Tunn. Undergr. Sp. Technol. Inc. Trenchless Technol. Res. 21 (2006) 384, https://doi.org/10.1016/j.tust.2005.12.195.
[38] M.W. Aleksander Urbanski, Karol Ryz, Przemyslaw Milczarek, Design of a railway overpass of soil-shell sheets. Analytical and numerical approach, Tech. Journal. Environ. (2012).
[39] T. Zimmermann, A. Truty, A. Urbanski, K. Podles, ZSoil user manual, Zace Serv. Switz. (2016).
[40] D. Łydżba, A. Różański, M. Sobótka, D. Stefaniuk, G. Chudy, T. Wróblewski, Mechanical behavior of soil-steel structure subjected to live loads and different water conditions, Arch. Inst. Inżynierii Lądowej. (2017).
[41] L. Pettersson, H. Sundquist, Design of Soil Steel Composite Bridges, KTH Royal Institute of Technology, 2014.
[42] L. Czesław Machelski, Janusz, The vehicle impact on the corrugated steel shell in soil-steel structures, Transp. Overv. (2017) 18–29, https://doi.org/10.35117/A_ENG_17_09_03.
[43] H.N. Kung, H.S. Lau, the Effect of Spacing on the Perform Ance of Soil-Steel Structures, University of Windsor, 1985.